Neural Co-Processors for Restoring Brain Function: Results from a Cortical Model of Grasping

Matthew J Bryan[1], **Linxing Preston Jiang**[1], **Rajesh P N Rao**[1]

[1] Neural Systems Laboratory, Paul G. Allen School of Computer Science & Engineering, University of Washington, Box 352350, Seattle, WA 98105, USA

E-mail: {mmattb,prestonj,rao}@cs.washington.edu

November 2022

Abstract. *Objective* A major challenge in closed-loop brain-computer interfaces (BCIs) is finding optimal stimulation patterns as a function of ongoing neural activity for different subjects and for different objectives. Traditional approaches, such as those currently used for deep brain stimulation (DBS), have largely followed a manual trial-and-error strategy to search for effective open-loop stimulation parameters, a strategy that is inefficient and does not generalize to closed-loop activity-dependent stimulation. *Approach* To achieve goal-directed closed-loop neurostimulation, we propose the use of brain co-processors, devices which exploit artificial intelligence (AI) to shape neural activity and bridge injured neural circuits for targeted repair and rehabilitation. Here we investigate a specific type of co-processor called a "neural co-processor" which uses artificial neural networks (ANNs) and deep learning to learn optimal closed-loop stimulation policies. The co-processor adapts the stimulation policy as the biological circuit itself adapts to the stimulation, achieving a form of brain-device co-adaptation. We tested the neural co-processor's ability to restore function after stroke by simulating a variety of lesions in a previously published cortical model of grasping. We additionally tested the ability of our co-processor to adapt its stimulation as the simulated cortical network and simulated sensors underwent changes. *Main results* Our results show that a neural co-processor can restore reaching and grasping function after a simulated stroke in a cortical model, achieving recovery towards healthy function in the range 75-90%. Our co-processor successfully co-adapted to accomplish the reach-and-grasp task after a variety of lesions to the simulated cortical circuit. *Significance* Our results provide the first proof-of-concept demonstration, using computer simulations, of a neural co-processor for activity-dependent closed-loop neurosimulation for optimizing a rehabilitation goal after injury. Our results provide insights on how such co-processors may eventually be developed for *in vivo* use to learn complex adaptive stimulation policies for a variety of neural rehabilitation and neuroprosthetic applications.

Keywords: brain-computer interface, neural co-processor, AI, machine learning, deep learning, neural networks, stimulation, computational models

1. Introduction

Brain-computer interfaces (BCIs) have made significant advances over the last several decades, leading to the control of a wide variety of virtual and physical prostheses through neural signal decoding [1, 2, 3, 4]. Separately, advances in stimulation techniques and modeling have allowed us to probe neural circuit dynamics (e.g. [5]) and learn to better drive neural circuits towards desired target dynamics by encoding and delivering information through stimulation [6, 7, 8, 9, 10, 11, 12, 13]. Bi-directional BCIs (BBCIs) allow stimulation to be conditioned on decoded brain activity and encoded sensor data for applications such as real-time, fine-grained control of neural circuits and prosthetic devices (e.g., [14]).

Motivated by these advances, we investigate here a flexible framework for combining encoding and decoding using "neural co-processors" [15], a type of brain co-processor [16]. Neural co-processors leverage artificial neural networks (ANNs) and deep learning to compute optimal closed-loop stimulation patterns. The approach can be used to not only drive neural activity toward desired activity regimes, but also to achieve task goals external to the subject, such as finding closed-loop stimulation patterns for motor cortical neurons for restoring the ability to reach and grasp an object. Likewise, the framework generalizes to stimulation based on both brain activity and external sensor measurements, e.g., from cameras or light detection and ranging (LIDAR) sensors, in order to restore perception (e.g., cortical visual prosthesis) or incorporate feedback for real-time prosthetic control (see [16] for details).

The co-processor framework also allows co-adaptation with biological circuits in the brain by updating its stimulation policy, while the brain updates its own response to the stimulation via adaptation and neural plasticity, or updates due to other reasons. This allows the co-processor to continually optimize its outputs for the desired optimization function in the presence of significant non-stationarity in the brain.

Here we use computer simulations to demonstrate a neural co-processor that restores movement in a computational model of cortical networks controlling a limb, after a simulated stroke affects the ability to use that limb. Our demonstration combines:

- An emulation model based on ANNs, which models the relationship between stimulation, decoded brain activity, and task performance.
- An AI agent based on ANNs which determines the best stimulation to apply in a closed-loop fashion in real time.

2. Background

Significant advances have been made in understanding and modeling the effects of electrical stimulation on the brain. Researchers have explored how information can be biomimetically or artificially encoded and delivered via stimulation to neuronal networks in the brain and other regions of the nervous system for auditory [6], visual [7], proprioceptive [8], and tactile [9, 10, 11, 12, 13] perception. Advances have also been

made in modeling the effects of stimulation over large scale, multi-region networks, and across time [17]. Some models can additionally adapt to ongoing changes in the brain, including changes due to the stimulation itself [18]. For our simulations described below, we use a stimulation model, not unlike those cited above, which seeks to account for both network dynamics and non-stationarity. In addition to training the model to have a strong ability to predict the effect of stimulation, we additionally adapt it to be useful for learning an optimal stimulation policy, a property distinct from predictive power alone.

Researchers have also explored both open- and closed-loop stimulation protocols for treating a variety of disorders. Open loop stimulation has been effective in treating Parkinson's Disease (PD) [19], as well as various psychiatric disorders [20, 21, 22]. In research more directly related to our work, Khanna et al. [23], investigated the use of open loop stimulation in restoring dexterity after a lesion in a nonhuman primate's (NHP's) motor cortex. The authors demonstrate that the use of low-frequency alternating current, applied epidurally, can improve grasp performance.

While open loop stimulation techniques have yielded clinically useful results, results in other domains have been mixed, such as in visual prostheses [24], and in invoking somatosensory feedback [13]. We believe this is due to the stimulation not being conditioned on the ongoing dynamics of the neural circuit being stimulated. From moment to moment and throughout the day, a neuronal circuit in the brain can be expected to respond differently even when the same stimulation parameters are used, due to the multitude of different external and internal inputs influencing the circuit's ongoing activity. Stimulation therefore needs to be proactively adapted in response. This need is even greater over longer time scales as the effects of plasticity, changes in clinical conditions, and ageing change the dynamics and connectivity of the brain. Closed-loop stimulation may also provide means to better regulate the energy use of an implanted stimulator, allowing it to intelligently regulate when to apply stimulation, in order to preserve implant battery life. Another benefit is that closed-loop stimulation offers an opportunity to minimize the side-effects of stimulation, through real time regulation of the stimulation parameters, such as in the use of deep brain stimulation (DBS) in PD patients [25]. In recent years, closed-loop stimulation has been used to aid in learning new memories after some impairment [26, 27], to replay visually-invoked activations [18], and for optogenetic control of a thalamocortical circuit [28], among others.

A major open question is: how does one leverage closed-loop control for real-time co-adaptation with the brain to accomplish an external task? "Co-adaptation" here refers to the ability of a BCI to adapt its stimulation regime to the ongoing changes in the circuit it is stimulating, and to adapt with that circuit to accomplish the external task (e.g., grasping). The neural co-processor we present here provides one potential model for accomplishing that. Through the use of deep learning, a neural co-processor model co-adapts its AI, which governs the stimulation, with the neural circuit being stimulated.

For a neurologically complex task such as grasping, it is not possible to design *a priori* a fixed real-time controller for the (potentially impaired) neural circuits involved in the task. That is due in large part to the variability of circuits from subject-to-subject, as well as variations in the placement of sensors and stimulators in the brain. The only plausible path to implementing a real-time controller is therefore to allow the device to adapt to the subject, long-term changes in their brain activities, and variability in the sensors, stimulators and hardware. Our proposed neural co-processors seek to accomplish such adaptation through ANNs and deep learning.

To gain insights into neural co-processors before testing them in *in vivo* experiments, we investigated a number of crucial design elements through the use of a neural network model of the cortical areas involved in grasping, presented previously by Michaels et al. [29]. We explored what properties of the co-processor allow successful adaptation to the short-term dynamics of the cortical model as it is being stimulated, as well as adaptation to longer-term connectivity changes in the cortical model. We present a training method for neural co-processors for learning optimal stimulation patterns that drive improvements in external task performance, while also adapting to the non-stationarity of the brain.

3. Methods

3.1. Architecture Overview

First, we present the architecture of our neural co-processor design. This design aims to solve two fundamental challenges in using neural stimulation to improve external task performance. First, to restore function for complex tasks, such as grasping, the mapping between neural activity, such as the activity encoding the intention to grasp, and the stimulation patterns to be applied to a downstream motor area to enable grasping cannot be pre-determined. As a result, the co-processor must learn what stimulation pattern is appropriate for achieving the external task. Unfortunately, in most cases, we do not know the optimal stimulation patterns to train the co-processor. This is because stimulation shapes the nonlinear dynamics of circuits in the brain in complex ways, leading to complex effects in external behavior. It is therefore not obvious what stimulation patterns will produce a desired behavior.

A neural co-processor attempts to solve these problems with a pair of artificial neural networks (ANNs) (Fig. 1):

- a "Co-Processor Network" (CPN), which maps neural activity, and possibly data from external sensors, to appropriate stimulation parameters.
- an "Emulator Network" (EN) which models the effect of stimulation on neural dynamics and behavior for the external task.

The CPN can be trained using the backpropagation algorithm, the workhorse of deep learning for training ANNs. However, backpropagation requires the error between the output of the CPN and a desired output, and as discussed above, we do not have

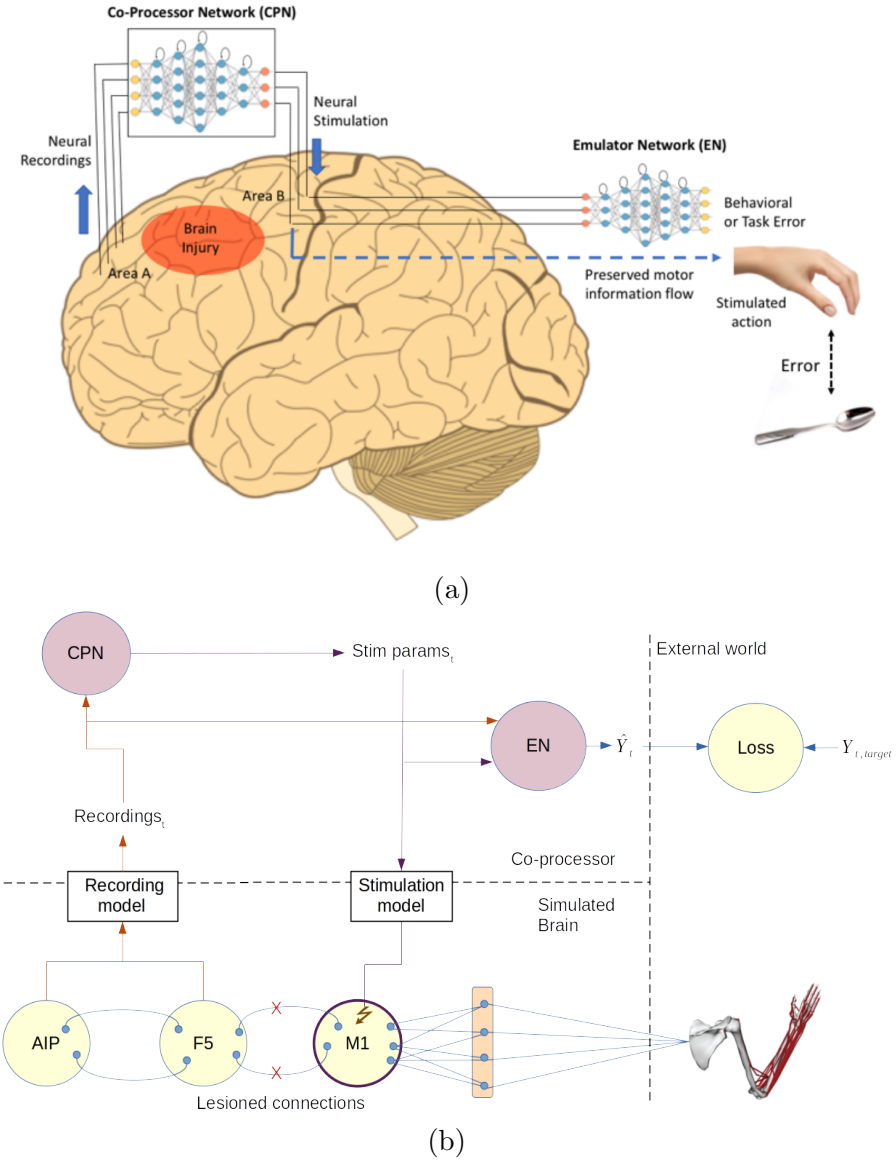

Figure 1: **Neural co-processor for restoring function after a brain injury**. An artificial neural network called the "Co-Processor Network" (CPN) is used to map input neural activity patterns in an area A to output stimulation patterns in same or other areas B in order to achieve a neural or behavioral goal using another ANN, an "Emulator Network" (EN) - see text for details. (a) The example here shows the CPN creating a new information processing pathway between prefrontal cortex and motor cortex, bypassing an intermediate area affected by brain injury (e.g., stroke). Adapted from [15], (b) Our current study involves a simulated cortical grasping circuit. The CPN and EN both receive simulated brain recordings, which are created according to a recording model (see Methods). The CPN outputs stimulation parameters, which are applied to the simulated grasping circuit, according to a stimulation model. The EN models the relationship between the stimulation, brain recordings, and external task.

the desired output stimulation pattern. We do however know what the desired output behavior in a task should be, e.g., a particular kind of grasp for a particular object or a particular type of neural activity in a brain area corresponding to healthy activity. We can therefore compute the error between this desired behavior and the actual behavior caused by the CPN due to stimulation. How do we backpropagate this error, which is external to the CPN, to update the parameters of the CPN?

We use a trained EN to backpropagate the external task error to the CPN. We train the EN to predict task-relevant parameters - a prediction of muscle velocities in our case - given the stimulation parameters output by the CPN and any measured neural activity. If the EN is trained to a sufficiently high level of precision, it can be used as a function approximator mapping stimulation to task output. When training the CPN, we treat the EN's output as the actual task output (e.g., actual grasp parameters). We backpropagate through the EN (without changing its weights) the error between the EN's output and the desired task output and use this backpropagated error to train the CPN (see Fig. 1).

In our experiments, the EN was a single layer fully connected long short-term memory (LSTM) recurrent neural network (RNN), with hyperbolic tangent (*tanh*) activations, and a linear readout. It has 87 LSTM neurons, which was chosen somewhat arbitrarily as a function of the input and output vector sizes. We found varying this neuron count did not drastically change results. Although other architectures could also be used, we found that this LSTM architecture allows the EN to continuously adapt to long-running dependencies in the simulated neural dynamics, ar better than a vanilla RNN. The CPN had an almost identical architecture, but with 61 LSTM neurons. As with the CPN, this neuron count was chosen as a function of the input and output vector sizes, but varying it upward had little effect on results. There is no requirement for the EN and CPN to have similar network architectures, but we found that these choices worked well in our experiments.

Note that the EN is more general than traditional models of neurostimulation which attempt to predict the effects of stimulation on *neural activity. The EN in a neural co-processor predicts the effects of stimulation (taking into account ongoing neural dynamics) on* task performance. This provides the key functionality needed to train the CPN. In the special case where the task involves driving neural circuits in the brain to desired neural activities, the EN reduces to more traditional models of stimulation.

For comparison, consider an EN architecture based on a traditional RNN with a nonlinearity. This is a nonlinear version of the common linear time-invariant state space model of stimulation (see, e.g., [17]). We found, however, that compared to LSTM-based EN, the linear model and the traditional nonlinear RNN are both not sufficiently powerful to capture the long-term dependencies in stimulation effects needed for the CPN to learn well. Our use of an LSTM-based EN builds on previous work modeling biological neural networks for predicting local field potentials [30], and modeling stimulation [31].

3.2. Simulation Overview

To test the feasibility of the neural co-processor approach, we used a previously published model of a grasping circuit in a nonhuman primate (NHP) brain. Using such a model allows us to explore some of the critical architectural choices and training algorithms, enabling us to rapidly and cheaply iterate on our design, prior to any *in vivo* experiments.

In the present study, we use the grasping network model of Michaels et al. [29] (Fig. 2a). The network, representing multiple interconnected cortical areas, was trained to mimic the grasping circuits of NHP subjects engaged in a delayed reach-to-grasp task. The model's design draws on a body of literature focused on architectures and training methods for RNNs which seek to create artificial neural networks with activation dynamics similar to biological circuits, including circuits for delayed grasping tasks [32]. The model consists of three "modular" vanilla RNNs (mRNNs), representing the cortical areas AIP, F5 and M1 respectively, and a linear readout layer (Fig. 2a). Each "module" consists of 100 vanilla RNN neurons, with a nonlinearity applied on the outputs. The modules are internally fully connected, and are connected to each other sparsely (10% connectivity in our case). The inputs to the network are visual features representing the object to be grasped, as well as a hold signal. The visual features intend to capture the features represented in the subject's visual cortex. They were extracted using VGGNet [33] from 3D renderings of the same objects which the subjects grasped. The hold signal is a boolean which encodes the point in the experiment when the subject began to reach. The outputs of the network are muscle length velocities for the shoulder, arm, and hand of the subject. The actual velocities were captured with a motion capture glove, and the Michaels et al. network model was trained to recapitulate those grasping motions.‡

The grasping model we use [29] implements a vision-to-grasp pipeline, from the visual processing needed to move the hand to the appropriate position for the grasp to shaping the hand for grasping an object of a particular shape. The emergent dynamics of the model's "modules", once trained, correspond roughly to the responses in the cortical areas AIP, F5, and M1 in a NHP subject's brain. Specifically, the activity of the first module (Fig. 2a), receiving the visual inputs in a trial resembles the activity in area AIP of the NHP subject from the same trial. Likewise, the second and third modules resemble the activity from the subjects's F5 and M1 cortical areas, respectively. The emergent network dynamics show a number of other correspondences to the subjects' brain activity as well (see [29] for details). For convenience, we will refer to the three modules in the model using the cortical areas (AIP, F5, M1) they correspond to. For details on how this network was trained, refer to Supplementary Materials 11.2. For additional details on the task structure, see Supplementary Materials 11.1.

An important attribute of the grasping network model is that the simulated circuit's activity shows a relatively clear separation for different object shapes, i.e. the visual

‡ Data and trained models from this work were supplied to us by the lead author of [29]. We re-implemented their model in PyTorch, and used their trained parameters for an arbitrarily chosen subject.

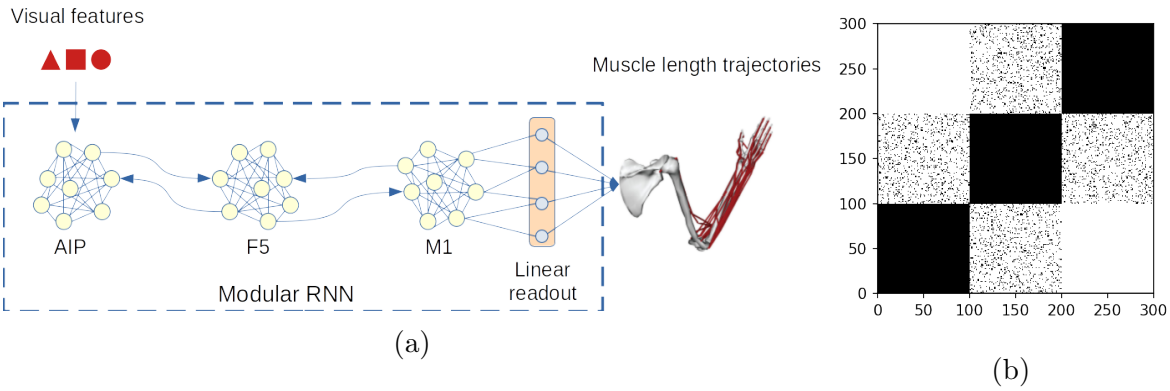

(a) (b)

Figure 2: **Architecture of the Brain Model.** (a) Modular RNN (mRNN) used by Michaels et al. [29] to model cortical circuits involved in grasping objects. The emergent dynamics of the three modules correspond well to neural activity in primate cortical areas AIP, F5, M1, respectively, for the same task. Visual features of an object (derived from VGGNet) propagate forward through the network, conditioning the grasp on the object's size and shape. (b) Connectivity matrix J. Connected neuron pairs are indicated in black, though the actual network weights are floating point values. White indicates non-connections. Note the within-module connections (black squares along the diagonal) are fully connected while connections to adjacent modules are sparse (10% of possible connections).

input to the network is leveraged by the model to successfully generate hand shape trajectories for grasping objects of particular shapes, and sizes. As we will note below, if the visual information is prevented from propagating through the modules, the model can at best learn a grasp stereotyped across all object sizes and shapes.

3.2.1. Lesioning the model causes real world failure modes. Simulating a brain lesion in the grasping model described above results in error modes which resemble some natural lesions of the primate brain. For example, a "lesion" involving zeroing some of the outputs of the first (AIP) module leads to a reaching motion generally succeeding, but finger muscle velocities show a high degree of error - effectively implying that the subject can reach to grasp, but cannot tailor the grasp to the current object. This is likely due to object shape information not being fully conveyed to the motor cortex (M1) module. Such a form of hand muscle spasticity is also a common symptom in certain strokes where the subject is able to position their hand, but is unable to properly form the appropriate grasp [23, 34].

On the other hand, if we lesion of a portion of the motor cortex (M1) module in the model, we see a more complete loss of movement, affecting even the ability to reach for the grasp. Finally, if we "disconnect" communication between the F5 and M1 modules, we see a failure similar to an AIP lesion: the reaching movement is generally achieved, but we see a disproportionate impact on forming the appropriate hand grasp. See Fig.

3 for examples.

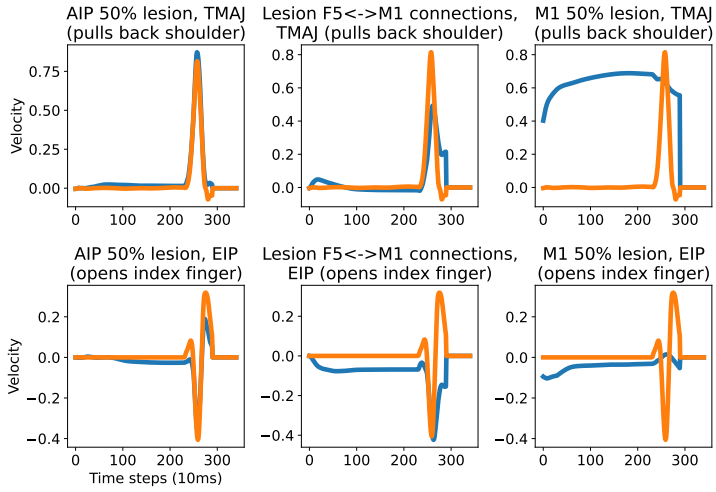

(a)

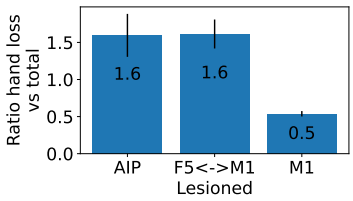

(b)

Figure 3: **Simulating strokes by lesioning different parts of the model lead to differential impact on grasping behavior.** (a) Example muscle trajectories before (orange) and after (blue) simulated stroke due to AIP, F5-M1 and M1 lesions for a shoulder muscle (top row) and a hand muscle (bottom row). Lesions which prevent a forward propagation of visual information tend to have a larger effect on hand pose (example EIP muscle shown) than on the shoulder, which is more involved in the reach motion (example TMAJ muscle shown). Lesions of M1 tend to cause a significant task loss on both. (b) Ratio of hand muscle mean squared error (MSE) losses vs. overall MSE losses, for different lesion types. The loss is measured relative to the model's movement trajectories prior to the lesion. Average of all trials, with +/- 1 stdev shown.

Given a particular type of lesion in the model, the co-processor's task is to generate the appropriate stimulation pattern given mRNN activities. The co-processor thus seeks to effectively bridge across the lesion and deliver stimulation to enable grasping behavior tailored to the current object's shape.

In our experiments, we studied our co-processor's performance on three types of simulated lesions:

- **Loss of AIP Neurons:** We force the output of some proportion of "AIP" neurons to zero, effectively removing them from the network. This results in some amount of loss of object shape information.
- **Loss of F5-M1 Connections:** We prevent the propagation of information between the "F5" and "M1" modules, effectively representing a severing of the connections between the two modules. Note that the connections are sparse and run in both directions, and we lesion the connections in both directions.
- **Loss of M1 Neurons:** We force the output of some proportion of "M1" neurons to zero. Here, the lesion may make it impossible for the co-processor to find a

perfect solution, since the loss of M1 neurons may make it impossible to activate muscles in the same ways. However, in Results we will see that some recovery is possible.

3.2.2. Simulated network exhibits long running and stable dynamics. To compute stimulation patterns that optimize for a task, the co-processor must learn to adapt to the dynamics of the network it is stimulating. Biological neural networks as well as our simulated grasping network exhibit long range changes in dynamics due to stimulation. A perturbation of the network (i.e. due to stimulation) will cause changes in neuronal activations long after the stimulation has been applied, sometimes far from the site of stimulation. Our model of the cortical grasping network exhibits the same behavior.

To illustrate this, suppose we apply a small, one-time perturbation to the hidden states of 10 randomly chosen neurons in the output (M1) module at some point in time during a trial. By repeating this experiment many times, we can understand what the distribution of long-running effects tends to look like on the output muscle velocities.

In Fig. 4 we see that even a single, one-time perturbation in the network has effects dozens of time steps later. Our co-processor will need to learn to take these dynamics into account. As we will show in the next subsection, the problem our co-processor faces in our simulations is in fact even harder than this since we also incorporate a model of stimulation effects on the neural circuit which includes both spatial and temporal smoothing.

3.2.3. Stimulation model. In our experiments, we stimulate neurons only in the output area (here M1) since the co-processor's purpose is to improve external task performance, which it is able to do with appropriate stimulation of the M1 output region of the network model. In a more general setting, it is conceivable that a co-processor could stimulate other areas of the brain as well to improve task performance downstream, or to probe the brain to better reveal the user's intent (i.e. object shape), but we leave these directions to future work.

To make our stimulation model more realistic, rather than allowing stimulation to directly change the output of single neurons, we simulated how stimulation may affect a network of neurons using a model that incorporates aspects of both spatial and temporal smoothing. Our intent was not to create a biophysical model of stimulation (our model does not arrange neurons in a volume to allow for such detailed simulation). Instead, the stimulation model approximates the effects of in-vivo biological stimulation (e.g. extracellular electrical stimulation) by diffusing the effects of stimulation across neural tissue space and time. Including this model implies that our EN must approximate this stimulation function, in addition to approximating the cortical dynamics of the brain and the mapping of those dynamics onto the grasping task. In Supplementary Materials 11.5, we compare results to the case with no stimulation or recording function.

Specifically, we use a stimulation function S which receives as input the stimulation parameter vector θ from the CPN. S performs temporal smoothing using a simple

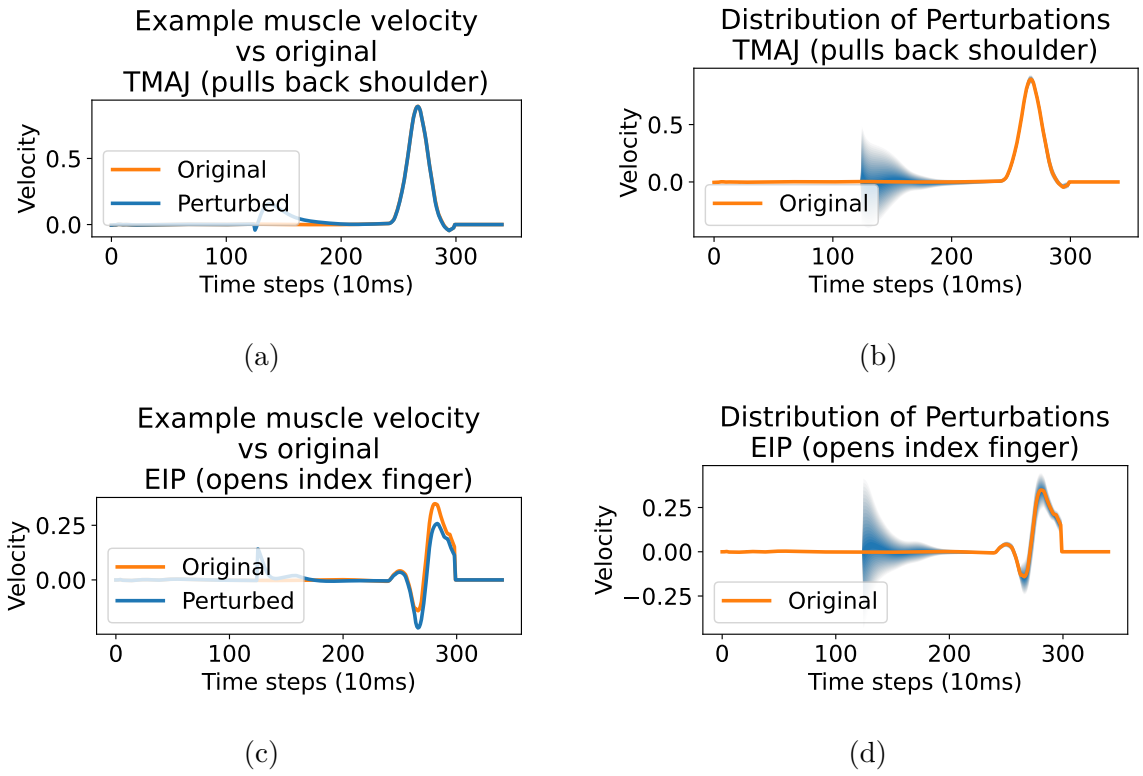

Figure 4: **Perturbations of the simulated cortical network (i.e. due to stimulation) have long-running effects on muscle activation.** Our results are consistent with the fixed point analysis of the network in [29], showing that the network exhibits stability. It tends towards the original trajectory after perturbation. Instantaneous random perturbation of a random group of 10 M1 neurons performed at time t=2s. (a, c) Single trial example for TMAJ, EIP muscles respectively. (b, d) Distribution of effects across n=1000 samples on TMAJ, EIP muscles respectively. Probability distribution shown to +/- 2 stdevs. Network exhibits similar behavior when perturbance is performed at other times.

exponential decay model by adding its current input to an exponentially decaying sum of inputs that decays towards 0.0 at some rate (see Equation 1 below). The effect of stimulation is thus not instantaneous, but rather decays with time. Likewise, to approximate how charge dissipates into a surrounding volume, we applied Gaussian smoothing to map θ (16-D in our experiments) to changes in the activations of a large number of the simulated M1 neurons (100 neurons in our experiments). If we assume each element of the θ represents the stimulation parameter for a single electrode, our Gaussian smoothing operation emulates how stimulation may affect the neurons in its vicinity more than it affects neurons further away. To accomplish that, we assume our model neurons are aligned along a spatial dimension arbitrarily and fix $\sigma = 1.75$.

The resulting equations defining our stimulation model are:

$$\alpha_t = \tau\alpha_{t-1} + \theta_{t-1} \tag{1}$$

$$s_t = C\alpha_t \tag{2}$$

- α: the 16 dimensional internal state of the stimulation function
- τ: our decay rate for temporal smoothing, which we set arbitrarily to 0.7
- C: a fixed 100×16 Gaussian smoothing matrix containing a single 1-D Gaussian in each column, to implement spatial smoothing and spread of stimulation to the stimulated neural population.
- s_t: the spatiotemporally smoothed stimulation vector whose elements denote how much stimulation is applied to each neuron at time step t (see Equation 3 below).

The governing equations of an mRNN with stimulation then become:

$$x_{t+1} = Jx_t + Iv_t + s_t + b \tag{3}$$

$$a_t = tanh(x_t) \tag{4}$$

$$y_t = La_t + l \tag{5}$$

- x: the hidden state of each model neuron
- J: recurrent weight matrix
- I: input weight matrix
- v_t: input
- b: activation bias
- L, l: parameters of the linear readout layer
- y_t: the output of the network

Fig. 5 depicts an example where θ is non-zero at $t = 0$ and zero for all other times, illustrating the effects of stimulation on the network across space and time. Fig. 6 illustrates the effects of stimulation during a stroke simulation. In this case, the trial is one where 50% of M1 neurons have been lesioned (their outputs are zero), the inputs to the CPN are from the AIP and F5 modules, and stimulation is applied to the M1 module.

3.2.4. Recording model. To simulate recordings of our model neurons, we used a recording model that assumed the model neurons are laid out along a single spatial dimension with the given number of electrodes spread evenly apart. We then applied Gaussian convolution, where the Gaussian kernel is centered at each electrode position. Thus, the recording from each 'electrode' is a Gaussian-weighted average of the activities of all neurons in the given module. Fig. 6 (bottom panels) show an example of recordings obtained using this recording model; note that the Gaussian-averaging of activities provides only a low-pass filtered, potentially ambiguous view of the activities of the underlying neurons, making it more challenging for the co-processor to interpret the neural activity and produce an appropriate stimulation pattern. Our simulated recordings are similar in spirit, though not actually modeling, local field potentials

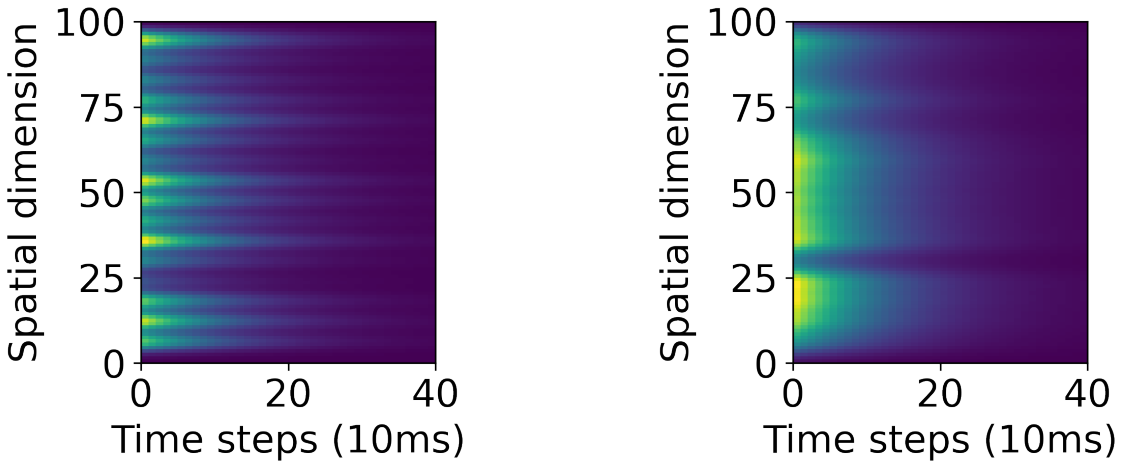

(a) $\sigma = 1.875$ (b) $\sigma = 2.875$

Figure 5: **Simulating the effects of stimulation on a recurrent network across space and time.** The stimulation model performs spatial and temporal smoothing of a 16-dimensional vector of stimulation parameters θ onto 100 neurons in a recurrent network. The 16 elements of the vector represent in-effect 16 electrodes located evenly along a spatial dimension, along which the 100 neurons are arranged arbitrarily. We show here the effects of two randomized θ with two respective smoothing parameters σ. After $t = 0$, θ is the zero vector. Color values indicate the magnitude of the value summed into each neuron's hidden state at that time step.

recorded extracellularly in biological neural tissue. In Supplemental section 11.6 we show that as we vary the observability of the brain via this recording model the results are largely the same, up to a point where objects can no longer be distinguished by the recording data.

3.2.5. Simulating co-adaptation by the brain. To demonstrate the co-processor's ability to adapt with the brain as it adapts to the co-processor's stimulation, we modify the cortical grasping network's parameters (synaptic weights and biases) throughout the co-processor's training. We use the standard error backpropagation algorithm to adapt the grasping network (using PyTorch's implementation of the *AdamW* optimizer). With each trial, task loss is calculated and backpropagated through the mRNNs as they receive stimulation. The learning rate was set arbitrarily to a relatively low rate of 1e−7 so that the network adapts more slowly than the co-processor.

3.2.6. Simulating recovery prior to co-processor use After a stroke, the human brain has the ability to learn and recover to some extent the behaviors affected by the stroke. We simulated this ability in our grasping network model by re-training the network for the grasping task after lesioning it. For our simulated lesions which zero the outputs of

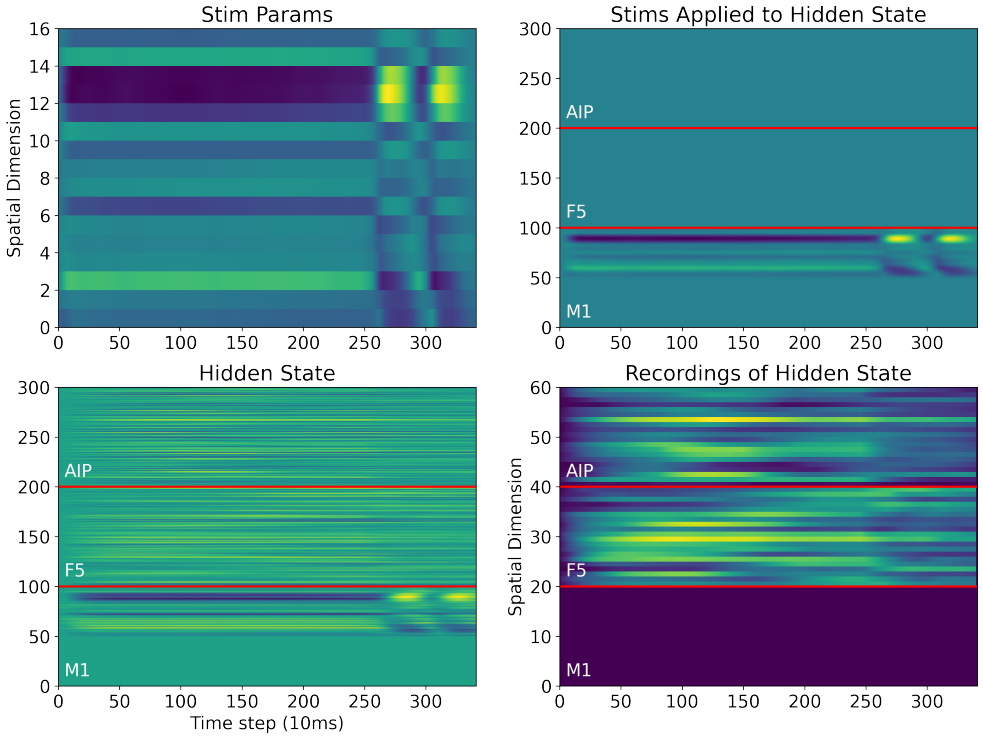

Figure 6: **Example of stimulation and recording for a single trial.** Here, M1 has been lesioned 50%, indicated by hidden states of M1 neurons with a value of zero (bottom left panel, lowest part of the plot) . We record neural activities (recording model) only from the AIP and F5 modules, as explained in Section 3.4. Stimulation is applied to M1 to drive the network's output. Stimulation is mostly constant until approximately t=275, when the hold signal was lifted and reach began.

neurons, the mRNN often cannot supply a partial recovery model. This is because the mRNN model has sufficient redundancy built into it that lesioning it by inactivating large numbers of neurons often leaves enough remaining degrees of freedom that a nearly full recovery can occur, unless so many neurons are lesioned that no stimulation could be effective.

In the case of a lesion that prevents communication between the F5 and M1 modules, information about the input object's shape cannot propagate forward in the network to allow shaping of the hand for grasping. However, the mRNN can learn a stereotyped grasp during the recovery period. After this recovery period, a co-processor can further boost grasp accuracy by forward-propagating object shape information from AIP and F5 to M1, acting as an artificial neural bridge. We explore this application of the co-processor in one of our experiments below.

3.2.7. Simulating a non-stationary recording function, e.g. sensor drift We also demonstrate the co-processor's ability to adapt to non-stationarity in the recording function. Over time, implanted sensors may drift from true readings. To test the co-processor's ability to adapt to that drift, we perform an experiment where the observation function has a bias term which changes over time, according to a random process. Each epoch, we add a random value to each element of the bias, drawn from a mean-0 Gaussian distribution. That causes the "sensors" to have a drifting zero point over time. See Supplementary Materials 11.4 for further details.

3.3. Training Paradigm

To train the CPN to generate appropriate stimulation patterns for grasping a given input object of a particular shape, we can use the backpropagation algorithm to minimize the errors between the current generated grasp and the desired target grasp. However, this error is in terms of grasp error instead of error in stimulation patterns (which is what the CPN needs), and we have no way of backpropagating grasp error through biological networks in the brain. This motivates our use of the EN as a model for the transformation from stimulation to muscle velocities: we backpropagate grasp error through the EN, while keeping its parameters fixed, and use this backpropagated error to change the parameters of the CPN towards minimizing grasp error.

Using the EN to train the CPN requires careful interleaving of EN and CPN training epochs. EN training epochs concentrate on updating the EN, based on observations of the effect of stimulation on the grasping network model's output. The loss function when training the EN is the mean squared error (MSE) loss between the EN's prediction and the actual output of the grasping network (i.e. muscle velocities). During the CPN training epochs, we keep the EN's parameters fixed and use the EN to train the CPN. Specifically, we backpropagate the MSE loss between the EN's predicted output, and the desired output (target muscle velocities for grasping the input object) through the CPN. Fig. 7 illustrates the EN and CPN training processes.

3.3.1. Training and testing data sets. For training and evaluation of our model, we use the same data as in Michaels et al. [29], which was provided to us by the lead author. The data consist of:

- The input visual features and hold signal. We input these to the simulated cortical circuit;
- The object identity. We use this to calculate how well the co-processor can differentiate objects; see Results section below;
- The muscle velocity data for the trial, as extracted from the data glove during the NHP trial, and as processed. This is our target output.

For each training session, we hold out a random sample of 20% of the data to act as our validation data set; we use the other 80% for training.

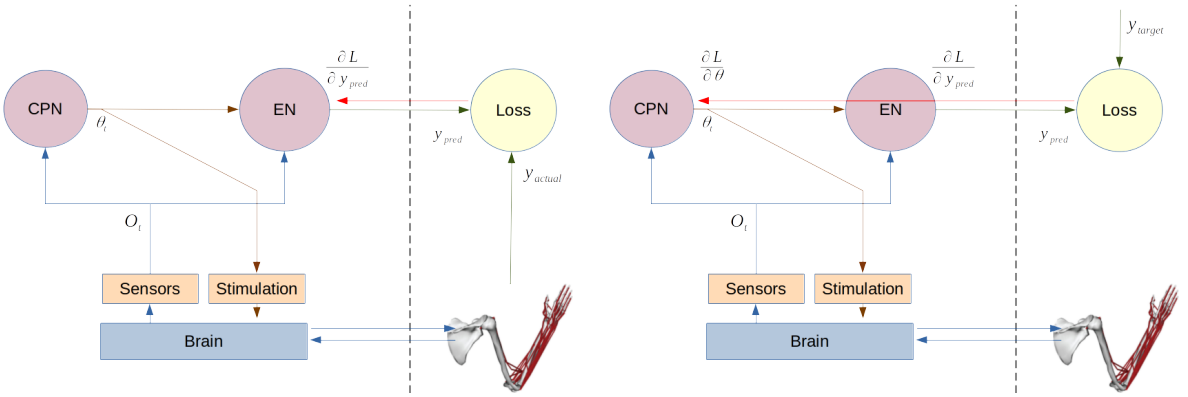

(a) (b)

Figure 7: **Training the neural co-processor.** (a) EN training phase: backpropagate actual vs predicted muscle velocity MSE loss. (b) CPN training phase: backpropagate actual vs target MSE loss, via EN, to CPN. This effectively treats the EN output as the actual, and thus the EN must be trained first.

3.3.2. EN training. For the EN to be useful for training the CPN, it must accurately predict the behavioral effects of stimulation produced by the CPN. In addition, backpropagating through the EN must yield gradients which are useful for changing the weights of the CPN in order to produce better stimulation patterns or minimizing the error. We discovered that this latter property does not occur simply by virtue of the former. Specifically, an EN can be trained to high levels of predictive power, even for random stimulation, and to orders of magnitude lower loss than the task loss, but backpropagation through the EN can still yield gradients which lead to unstable training of the CPN.

We hypothesize that the crux of the EN training problem is one of over-fitting: the EN may be trained to achieve high predictive power on a data set of stimulation examples, but due to the high dimensionality of our stimulation parameters θ, and the dynamics of the network being stimulated, the function learned by the EN may be biased and provide gradients not suitable for the stimulation inputs generated by the CPN during its training.

To address this problem, we first structure the training dataset for each EN training epoch in a specific way. Each epoch, we include:

- training examples using stimulation inputs generated by the current CPN;
- training examples using stimulation inputs generated by a small collection of CPNs obtained by adding zero-mean Gaussian noise to the current CPN's parameters; and
- training examples with white noise stimulation inputs.

Such a training paradigm is designed to cover a sufficient variety of examples to prevent overfitting, and to do so in a way that explores the neighborhood of the current

CPN's parameter space. Augmenting a CPN-generated data set with white noise examples alone was not sufficient to stabilize CPN training, but including additional examples generated by CPNs in the neighborhood of the current CPN helped train the EN to perform well in that neighborhood and produce useful gradients for the CPN. "Neighborhood" here refers to the region of CPN parameter space near the current CPN. This may cause the EN to be overfit, i.e. fit to the local area of CPN parameter space but exhibiting poor predictive power in other areas of the space. However, we solve this problem by retraining the EN, interleaved with CPN training. We show the effect of this dataset composition in one results section below (4.3).

We composed each batch of EN training data as follows:

Source	**Proportion of dataset**
Data from current CPN	10%
Data from current CPN with parameter noise	60%
Data from white noise stimulation	30%

Additionally, we use decoupled weight decay regularization [35] to mitigate overfitting, and a carefully chosen learning rate schedule. The schedule begins with a higher learning rate initially (4e−3), ramping down to a lower rate (1e−4). The learning schedule is based on the most recent prediction error on the validation portion of the data set. We found that using rates much lower or higher than these rates in any training phase may cause the EN learning to not converge. EN training proceeds until the network's output error exceed a threshold, defined as a fraction of the current CPN's task loss. See Section 3.3.4 for further details on when we switch between training the EN and CPN.

3.3.3. CPN training Once an EN is properly trained, we can use the EN as a surrogate for the part of the grasping model that transforms stimulation patterns and neural activity to grasping behavior. We use a large number of randomly sampled trials from the original Michaels et al. task [29] and generate stimulation patterns using the current CPN alone. These stimulation patterns are passed through the EN to generate predictions of output muscle velocities, which are compared to the desired target velocities to compute the error. We backpropagate this error through the EN (without modifying its parameters) to generate training gradients for the CPN. Fig. 7 illustrates this training process.

We found that the CPN appears to train in two phases. In the first phase, it is largely learning the structure of the reach-to-grasp task, e.g. that the muscles need to remain at a position during the hold period until the reach begins. During this early training phase, the learning rate can be quite high (1e−3). Later, the CPN begins to learn the mapping between object shape information and the stimulation patterns needed to approximate the target grasp for that object. This later phase of training requires a learning rate 2-3 orders of magnitude lower than in the first phase (1e−6 − 5e−5). See Section 4 for more details.

3.3.4. Interleaved CPN/EN training, and adapting to non-stationarity Having defined the training procedures for the EN and CPN, we can define a training algorithm combining those two. We train the two in alternation, creating a new EN each time we enter an EN training phase. We explored the possibility of reusing an existing EN but found that retraining an EN was no more fast than training a new one. Training a new EN also allows us to adapt to the brain's non-stationarity. That requires us to determine when the current EN is no longer suitable for training the current CPN. Our algorithm retires the current EN and trains a new one when one of two conditions is satisfied: (1) the EN's prediction error is sufficiently above some fraction of the CPN's task loss; or (2) if CPN loss does not improve (or gets worse) over a sufficient number of recent training steps (this is a common stopping criterion in machine learning). Additional details can be found in the Supplementary Materials section 11.3.

3.4. Experiments

We performed 8 experiments to investigate the co-processor's ability to learn under a variety of conditions: we studied three types of lesions to the grasping network (simulated stroke) and for each lesion type, we either turned on or off brain co-adaptation, natural recovery before co-processor use, and non-stationarity due to sensor drift. The following table summarizes the experiments (a blank entry under a condition (e.g., Simulate co-adaptation?) means "No" while an X means "Yes"):

	Lesion	**Simulate co-adaptation?**	**Simulate recovery?**	**Simulate sensor drift?**
1	50% AIP loss			
2	50% AIP loss	X		
3	50% M1 loss			
4	50% M1 loss	X		
5	100% connection loss F5<->M1			
6	100% connection loss F5<->M1	X		
7	100% connection loss F5<->M1	X	X	
8	100% connection loss F5<->M1	X		X

For each experiment, we used the mRNN grasping model from Michaels et al.[29], and the same set of input and output data used in their work. The dataset contains a total of 502 trials, sampled uniformly across 42 object classes. In each experiment, we held out a random sample of 20% of the dataset for validation.

3.5. Stopping condition

In these experiments, we train the co-processor until one of two conditions is satisfied:

- The percent change in average task loss between two consecutive ranges of 500 epochs is below a threshold of 0.01%, indicating minimal benefits of further training.
- We have exceeded 250k epochs, which acts as a hard stopping criterion.

4. Results

For each lesioning experiment, we track two metrics to characterize the learning progress. First, we track the task loss, which is an MSE loss that measures the co-processor's ability to restore movement towards the target trajectory. We define it over the muscle length trajectory vector output from the lesioned grasping network model, compared to the ground truth muscle length data captured during the Michaels et al. experiment [29]. In graphs, we characterize this loss in terms of percent recovery - i.e. difference between lesioned and healthy performance. Figs. 8-13 and Table 2 provide the detailed results.

Second, we measure the degree to which lesioned grasping network, when coupled with the co-processor, successfully differentiates object classes. We compared the ratio of within-class to total variation between the lesioned and the healthy network. This metric S is defined as:

$$S = \frac{\sigma_a}{\sigma_w} - \frac{\sigma_{a,h}}{\sigma_{w,h}} \tag{6}$$

where σ measures the mean variation, across time, and across all data points in a given sample, σ_a is the total variation of a dataset, and σ_w is the average of the within-class variations (h indicates healthy). An S value of 0.0 indicates that the grasps for the different object classes vary to the same degree as the healthy network.

The metric S allows us to differentiate overall task performance improvement and the ability of the co-processor to condition the grasp on the input object based on visual information. To successfully grasp in the real world, the hand must be preformed appropriately for the shape of the object being grasped, and must close around it appropriately. Note that the structure of the delayed reach-to-grasp task can potentially be learned by the co-processor, (e.g. to hold muscle velocities to 0.0 for the initial part of each trial) without the co-processor also learning to differentiate the various object shapes from the brain observations. Thus, S is useful for differentiating improvement in object differentiation as opposed only overall decrease in task loss.

4.1. Experiment 1: AIP 75% lesion

Our first experiment tested the ability of the co-processor to compensate for the loss of a significant fraction of neurons in the area AIP of grasping model, which is responsible for encoding object shapres from visual inputs. Loss of AIP neurons results in the network model, without further adaptation, being unable to condition its grasp on the object

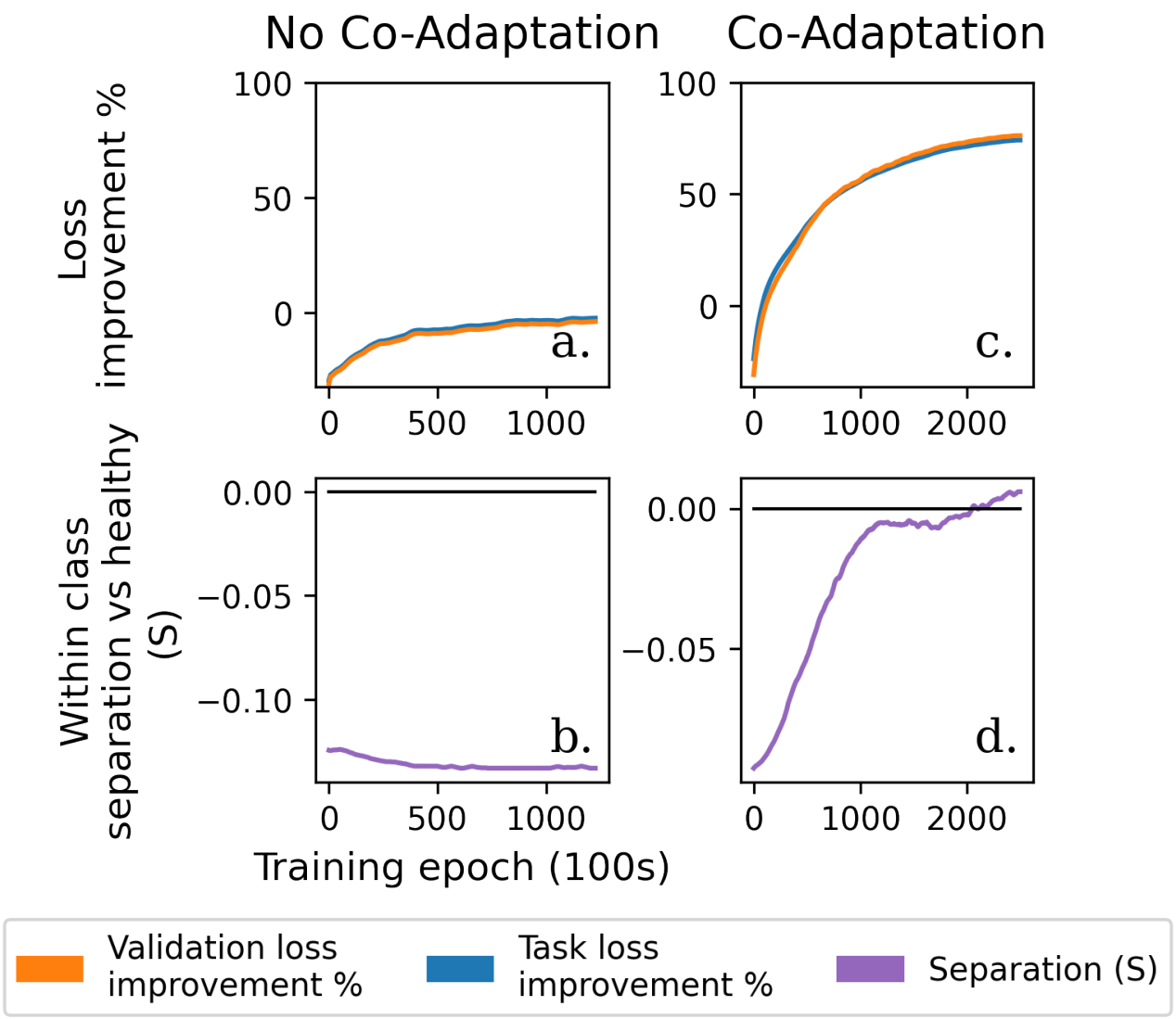

Figure 8: Training Results: AIP 50% Lesion

shape, after largely succeeding in reaching toward the object.§ See Fig. 8a. Likewise, the co-processor cannot observe the object shape encoding in the brain, because that encoding is no longer happening. As a result, further recovery is not possible. Note in Fig. 8b that the co-processor never learns to separate object classes, which would have been indicated by an S value near 0.0.

In the co-adaptive case, the brain and co-processor find a solution that reaches 76% recovery towards non-lesioned performance. This demonstrates that the co-processor can adapt to the non-stationarity of the mapping between the observed brain activity and the CPN-delivered stimulation. As the brain adapts, it learns to encode the input

§ Note in Supplementary Materials 11.7 that lesioned loss is lower in this experiment than in others: the user continues to reach successfully, but not to form the hand properly, as explore above. Likewise, the co-processor doesn't have sufficient information to improve performance, for lack of that information.

visual information, which in turn allows the co-processor to observe that information through brain recordings. The co-processor can then leverage that information to condition stimulation. See Fig. 8c. Note, though, that the simulation is not designed to indicate if the co-processor speeds up recovery, or provides better results than natural recovery, since we aren't modeling the timeline of natural recovery. With this lesion design, simulated recovery would in-fact allow near-complete recovery of task performance. As a result, this experiment intends only to demonstrate co-adaptation.

In Fig. 8d, which plots the object separability metric S discussed above, we see that initially the co-processor and brain do not strongly separate the object classes, resulting in negative S values, but as the training proceeds, the metric exceeds 0.0, indicating separability. This can be attributed to the co-processor and the simulated "brain" learning how to map the input visual information about object shape to the appropriate grasp for the object.

In Figs 8a and c, we see the co-processor initially causes worse performance, as indicated by the negative recovery rate. At this point the CPN is newly initialized, and has therefore not yet learned an interpretation of the recordings, or the problem structure.

4.2. Experiment 2: M1 50% lesion

In this experiment, we lesioned 50% of the M1 module of the grasping network model. In the non-coadaptive case, training quickly plateaus at 75%, and does not improve thereafter. This suggests the lesion inactivated some of the degrees of freedom needed to control the output layer, resulting in a reduced ability to recreate the different target grasps for different objects. See Fig. 9a.

In the co-adaptive case, performance likewise hits an inflexion point at 75%, but continues to improve slowly. The ability to improve further is tied to the "natural" recovery occurring in the co-adapting network model, which restores some of the degrees of freedom needed for improving grasping performance. The co-processor in this case adapts successfully to this non-stationarity due to the recovery process. See Fig. 9c.

4.3. Experiment 3: F5 and M1 connection lesion

In this experiment, we disconnected F5 from M1 completely to test whether the co-processor can act as a bridge between the two areas to appropriately convey information required for the grasping task from one area to the other. As in the other experiments, the co-processor's loss in this experiment improved quickly, but took much longer to refine the stimulation patterns to enable object differentiation. See Fig. 10a and c.

Since feedback from the output cannot "backpropagate" to the F5 and AIP modules, co-adaptation and learning in this experiment only affects the M1 module. As a result, this experiment demonstrates that the co-processor's learning algorithm is capable of adapting to non-stationarity in the network model's mapping between stimulation parameters and the behavioral output (muscle velocities for grasping).

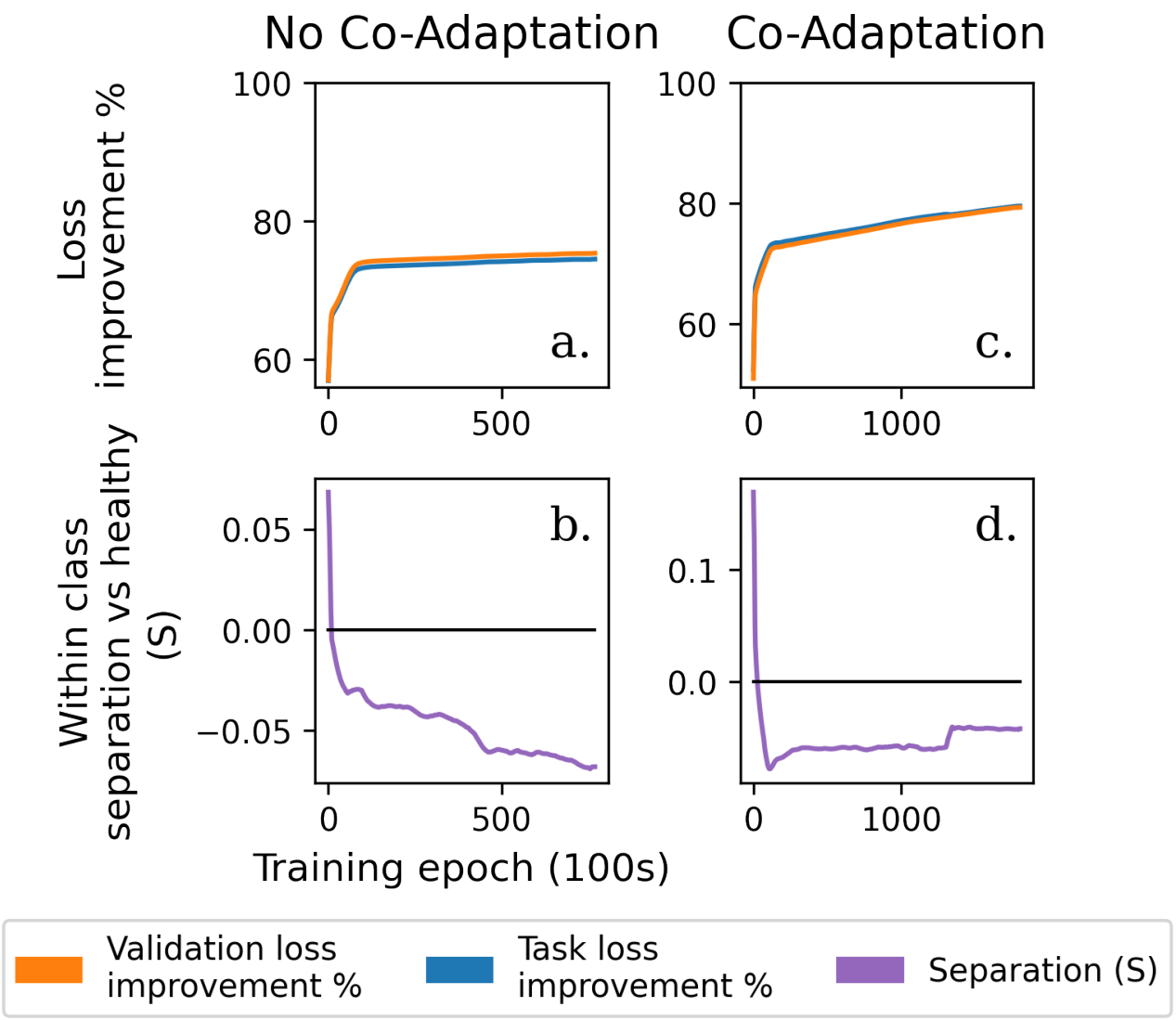

Figure 9: Training Results: M1 50% Lesion

These results contrast with the results of Experiment 1, where the non-stationarity affected the mapping between the visual inputs and the AIP outputs.

As seen in Fig. 10b and d, object separation is initially low and unstable, as the co-processor begins to learn the task. Afterwards, it stabilizes as the co-processor begins to leverage observed brain activity to differentiate object shapes, gradually converging towards the pre-lesion grasping performance.

To illustrate the effect of EN training data set composition as described in 3.3, we performed additional experiments where we vary the data set composition. We chose to base those experiments on the F5-M1 connection lesion arbitrarily. As outlined in Training (3.3), the training data set for the EN is composed of stimulation examples drawn from the current CPN, examples drawn from other CPNs with parameters in the neighborhood of the current CPN in parameter space (referred to as "exploratory

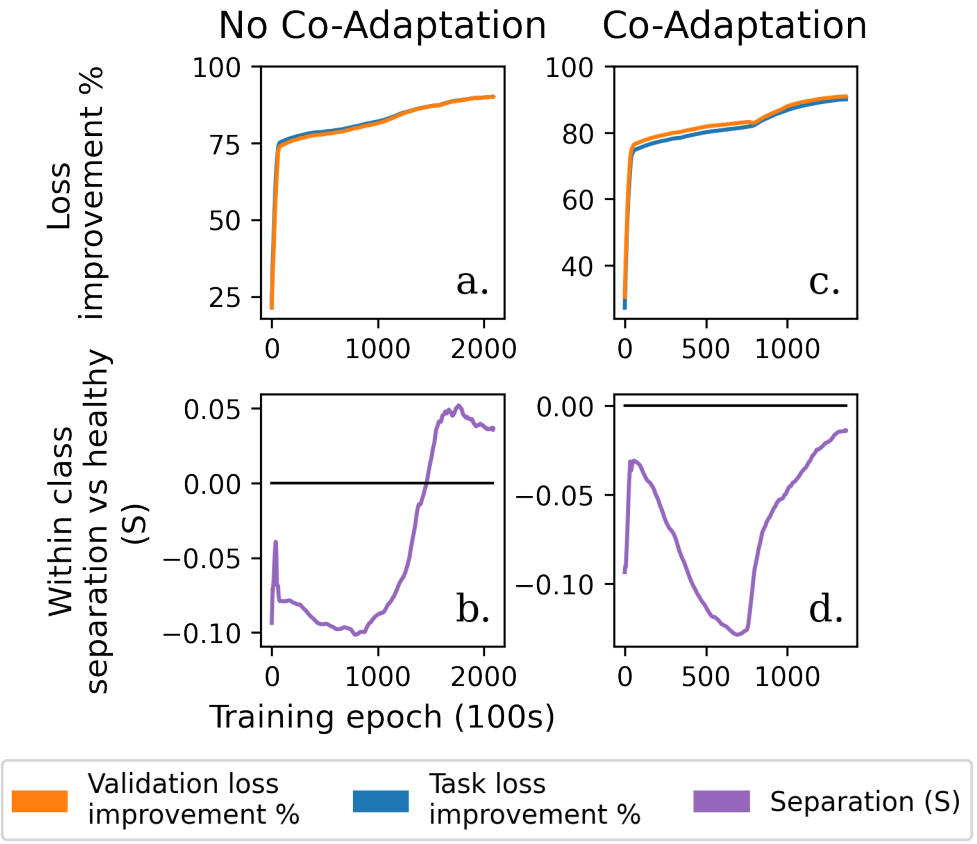

Figure 10: Training Results: F5-M1 Connection Lesion

examples"), and randomized stimulation. In Fig. 11 we see the effect of removing the latter two of those. Exploratory examples proved necessary to stabilize training, and to achieve higher levels of recovery, as in Fig. 11a. Removing the examples of randomized stimulation results in even more unstable training, where no improvement in task performance occurs.

4.4. Experiment 4: Connection lesion with recovery

It is often the case that after a stroke, the brain recovers some of the function lost immediately after the stroke. We simulated this recovery in the grasping network model after lesioning the F5-M1 connections by training the lesioned network on the grasping task. Complete recovery is impossible because the M1 module's connections to F5 (both forward and backward) are disconnected. The grasping network model in this case learns an object-agnostic stereotypical grasp. We tested whether a co-processor can improve grasping performance by propagating to M1 the object-related information from F5 necessary to tailor the grasp to the current input object's shape.

We found that the co-processor can successfully improve task performance beyond the "natural" recovery after stroke (Fig. 12a). The dashed line indicates the task loss after initial recovery. As in some experiments above, loss is initially higher at first, as

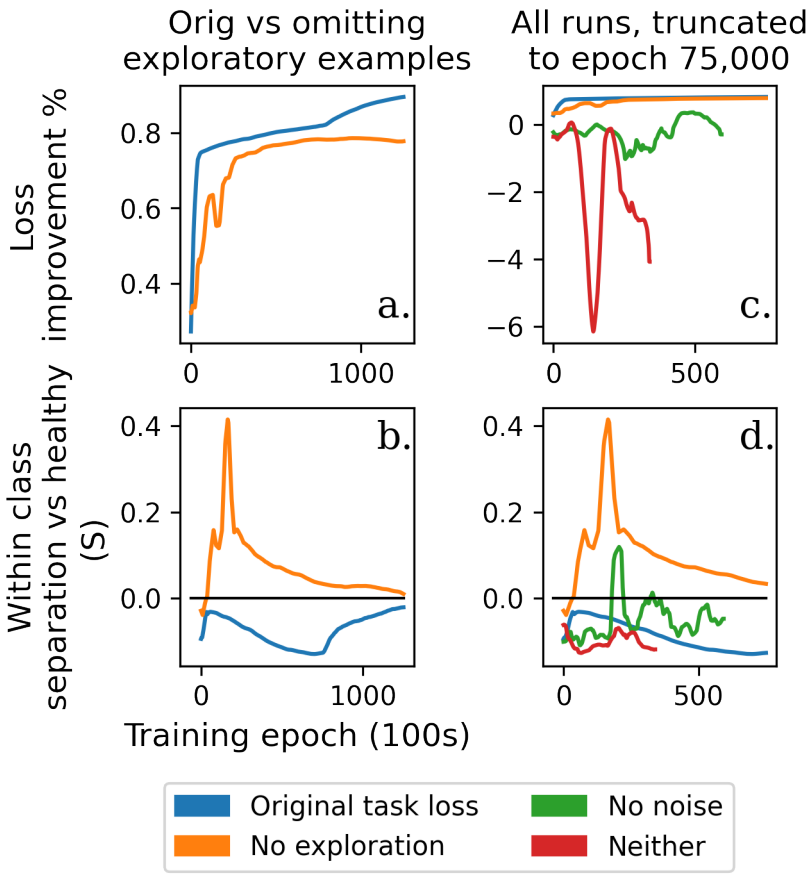

Figure 11: Training Results: F5-M1 Connection Lesion. Use of exploratory and randomized examples in the training data set lead to stabilized and faster training. (a) Without exploratory examples in the neighborhood of the CPN, we have unstable and slower training. In this case, the data set is composed of 10% examples drawn from the CPN, and 90% randomized examples (no exploration). (b) Using only examples from the CPN and/or exploratory examples also leads to unstable training. Here we additionally show experiments with 90% exploratory examples (no noise), and 100% examples drawn from the CPN (neither).

the co-processor trains. Eventually however it learns to drive the task loss lower, as it learns to forward-propagate information from the "earlier" parts of the simulated brain. Also, note the object class separation metric S returned to a healthy value towards the end of co-processor training (Fig. 12)b.

4.5. Experiment 5: Connection lesion with sensor drift

In our final experiment, we again lesioned the F5-M1 connections and allowed co-adaptation by the simulated model network but additionally, allowed the sensor readings to drift over time. This drift was modeled in the recording function, where the readings had a non-stationary zero point across epochs. We added a bias term which we updated

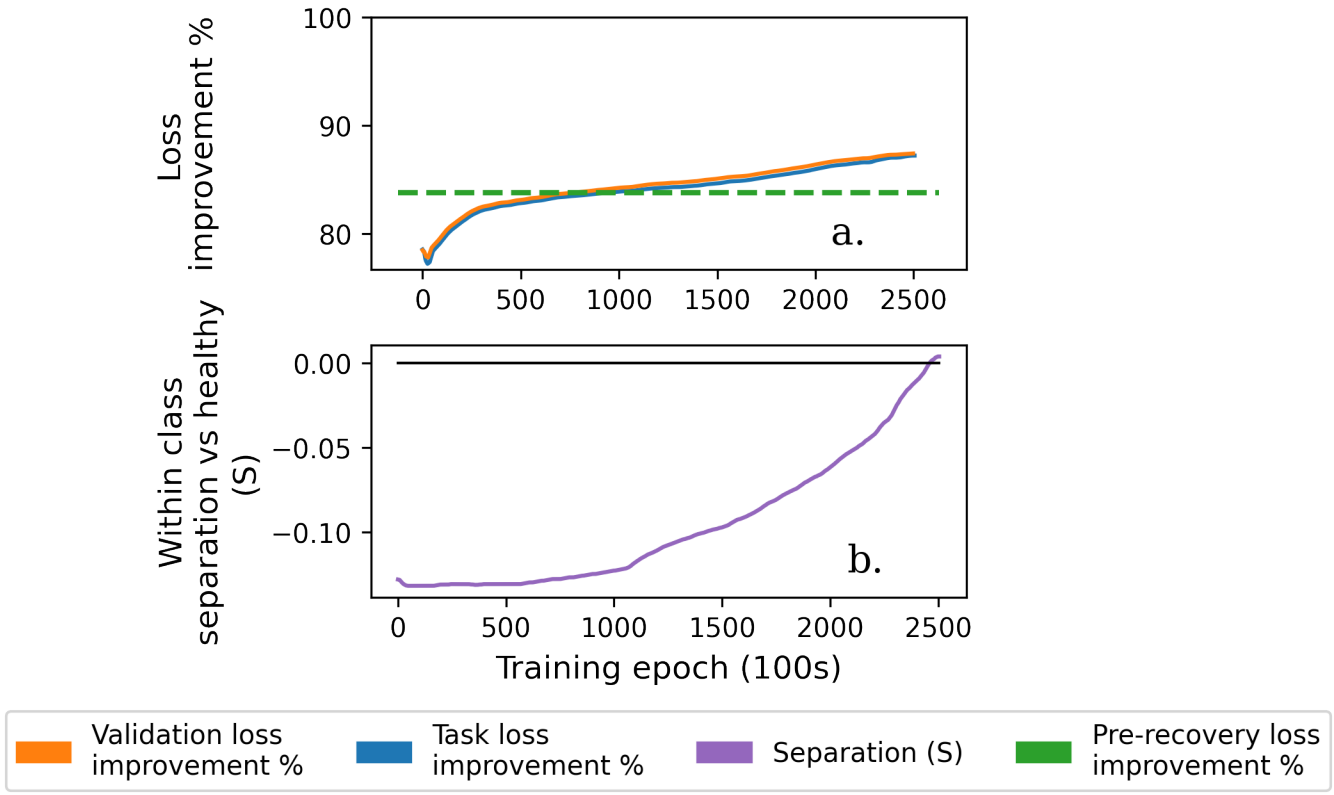

Figure 12: Training Results: Connection Lesion with Recovery

between epochs according to a random process. See Supplementary Materials 11.4 for details. Sensor-related non-stationarities are often seen in real-world neural recording systems due to a variety of factors, from impedance changes due to sensor movement to biological scar tissue formation.

As seen in Fig. 13, the co-processor was able to quickly recover the reach-to-grasp part of the task, and gradually learned to condition the grasp on the object information. Because the recording model is non-stationary in this experiment, the object class separation exhibits far greater epoch-to-epoch variance in the later epochs. The co-processor presumably becomes more reliant on upstream visual information over time, as it learns how to leverage this in order to differentiate object shapes.‖

As expected, training efficiency was decreased relative to the experiment without sensor drift: with the sensor drift, 282K training epochs was needed to reach 85% recovery while without sensor drift, only 93K was required.

‖ For this experiment, we opted to stop training after running the experiment long enough to get results near to the version of this experiment without sensor drift.

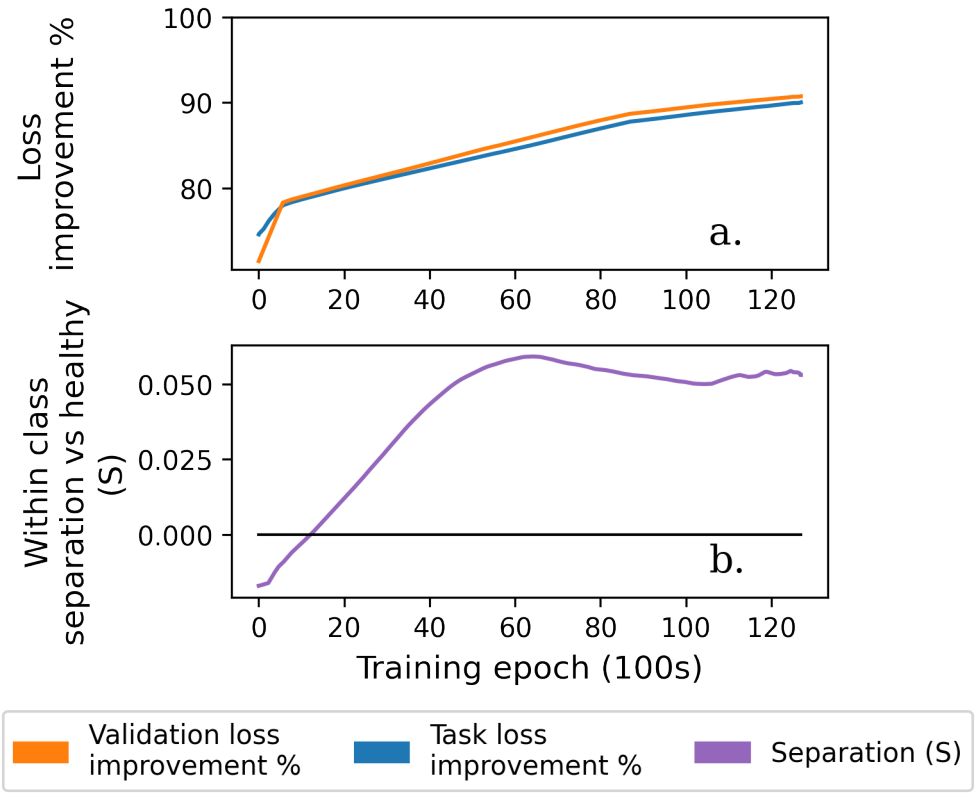

Figure 13: Training Results: Connection Lesion with Sensor Drift

5. Discussion and Future Work

We present here a first-of-its-kind demonstration of a novel design for neural co-processors, allowing for an AI agent to learn neural stimulation policies that improve a user's performance of an external task. The design revolves around the use of a stimulation model for training the agent, providing a proxy to the true function mapping stimulation and neural activity to task performance. We base our demonstration on a simulation of a neural circuit engaged in an external grasping task.

Our co-processor design adapts well to a variety of simulated lesion types, reducing task loss 75-90% across our various experiments. To work this well, the co-processor needed to adapt to the long-running dynamics of the simulated network, as well as the long-running effects of stimulation. In some experiments we required it to additionally adapt to non-stationarity in the neural circuit, which was actively changing at the same time the co-processor was learning, which it achieved as well. In one experiment, it also adapted to a simulated brain which had already undergone some amount of lesion recovery. In that case, the co-processor successfully identified the information upstream from the lesion which was necessary to stimulate the motor cortex (M1) module downstream. In the final experiment, it also successfully adapted to a non-

stationary recording model.

A previous example of such a simulation approach is the work of Dura-Bernal et al. [36]. In this work, the authors used a simulated spiking neural network to train a stimulation agent. Their stimulation agent sought to restore the network's control of a simulated arm to reach a target, after a simulated lesion was applied. As the authors point out, we have a limited ability to probe a neural circuit *in vivo* in order to perform learning. As a result, we first need to design our approach through the use of an admissible simulation. As we did, the authors in this case simulated lesions by effectively removing parts of their simulated network, or by cutting connections between parts of the network.

Clearly, we need to discuss what can and cannot be inferred from simulation studies such as these. We note that our simulation differs drastically from an organic brain, both in scale and structure. Today, predicting long-running neural responses to stimulation remains a difficult problem, implying targeted neural control is also difficult. Even more so, identifying the neural correlates of complex task success remains largely out of reach [23]. What, then, does our simulation provide us?

Our simulation does not constitute evidence that our method will, for example, immediately translate to true restoration of fine-grained control for individual fingers of a stroke patient. One clear challenge with doing so would be the sheer dimensionality of natural brain dynamics, and how that compares to the resolution of stimulation the co-processor can learn to apply. There exists a mismatch between the dimensionality of the underlying problem, sensor and stimulator technologies, and the amount of training data which can reasonably be collected to train a closed-loop neural controller. We argue that while this fact clearly creates a challenge for learning-based closed-loop stimulation, that nevertheless the insights we generate through this simulation are likely to be applicable.

First, this simulation requires the co-processor to contend with issues of long-running dynamics, high dimensionality, and non-stationarity, which are likely to be key issues facing real world deployments. We designed our training algorithm to contend with dimensionality by training the CPN with a local stimulation model. The algorithm adapts to non-stationarity by regularly updating that stimulation model, allowing it to adapt to changes in the brain, in addition to "following" the CPN through stimulation parameter space.

Second, the co-processor abstractly lends itself to any closed-loop neural stimulation problem where a relevant stimulation model can be identified. There are many lower dimensional problems today which we address with far simpler stimulation regimes than would be necessary for e.g. fine-grained finger control. In some applications, such as Parkinson's disease symptom relief, stimulation is often parameterized by a single off-vs-on parameter, or a small handful of parameters, where the key challenge is learning when to apply the stimulation, and its shape and power. Our simulation demonstrates the ability of our training method to adapt to higher dimensional problems than these, where additionally the long-running effects of stimulation on the intended figure-of-merit must be modeled. These properties together suggest it may be useful in lower

dimensional problems where a stimulation model can be estimated, and stimulation parameters can be tied to the target objective.

Our future work will include a reinforcement learning (RL) approach, where the co-processor explicitly learns when to apply stimulation, in addition to parameterizing it. Its target objective involves not only symptom relief, but also minimizing energy use. In this approach, our CPN and EN may correspond to the Actor and Critic portions of an Actor-Critic model for example. Here, the Critic would learn to value symptom relief, while attaching a cost to stimulation, thus incentivizing an energy efficient approach.

One challenge remaining with our current co-processor design is training efficiency. On the whole, the co-processor quickly improved task performance, but required orders of magnitude more training examples to achieve its highest levels of performance. Even moderate amounts of recovery may be valuable to a user, but nevertheless we consider training efficiency to remain a problem. Due to limits on patient fatigue, time, implant battery life, and other concerns, it is not plausible to expect a learning algorithm to have access to unlimited amounts of training data. As a result, it is necessary to make efficient use of the data we can acquire. We believe there exist at least three mitigations for that:

- Retraining an existing EN, rather than regularly creating a new one. As mentioned above, we encountered difficulty with this approach, but it remains to be seen if this is a fundamental problem with our training method, rather than a peculiarity of our simulation. Also, it remains unclear if a solution for our simulation exists as well, which we've simply yet to identify. This remains a future area of inquiry.
- Making better use of what data we acquire. In this initial simulation we do not retain data beyond the present training epoch because non-stationarity requires us to regularly discard or discount data as it ages. We found that in the presence of a rapidly learning CPN, and especially in our co-adaptive experiments, data retention in-fact caused training instability such that training eventually required more data collection than otherwise. However, in practice, training epochs operate on the order of seconds, suggesting that data can be retained and reused for multiple epochs. The 'speed' of non-stationarity compared to the co-processor's learning therefore is an area for future research.
- Matching the dimensionality of the stimulation and recording parameters to the amount of available data. A stimulation regime with a small number of controllable parameters that nevertheless allows improvements in task performance will likely require less training data.

Future work will test the neural co-processor framework on lower dimensional problems that are likely to transfer more readily to *in vivo* experiments and human trials. We hypothesize that the co-processor framework will transition well to treatments for conditions such as Parkinson's disease (PD), and essential tremor (ET). For example, Castaño-Candamil et al. [37] used an ML-based approach to closed-loop stimulation for ET where a simple learning model extracted neural markers (NMs) from a human

patient's M1 cortex and used the NMs to determine deep brain stimulation (DBS) stimulation parameters. Our co-processor model is likely to transition well to such an application by being able to extract neural markers appropriate for various contexts (e.g. sitting or standing) and applying stimulation appropriate to the current context.

6. Conclusion

Using a simulated model of circuits in the primate brain involved in grasping, we demonstrated that a closed-loop neural stimulator, called a "neural co-processor" can be trained to restore grasping function after different types of lesions to the model. We showed a neural co-processor can be trained using supervised learning through backpropagation with the help of two networks: a co-processor network (CPN) that learns to generate stimulation patterns to optimize task performance, and an emulator network (EN) that learns to predict the effects of stimulation. Our results show that a neural co-processor can improve task performance after a lesion by co-adapting with the simulated brain model in the presence of nonstationarities in the brain and sensors. Given the generality of the framework, we expect neural co-processors to be applicable to a wide range of clinical applications that required adaptive closed-loop neural stimulation.

7. Data availability statement

Code including analysis code used to generate figures can be found at `https://github.com/mmattb/coproc-poc`. Data is available upon reasonable request to the authors.

8. Conflict of interest statement

The authors of this work are not aware of any conflicts of interest related to it.

9. Acknowledgements

This work was supported by a Weill Neurohub Investigator grant, a CJ and Elizabeth Hwang endowed professorship (RPNR), and National Science Foundation grant no. EEC-1028725. The authors would like to thank Karunesh Ganguly (UC San Francisco), Priya Khanna (UC Berkeley), Anca Dragan (UC Berkeley), Justin Ong, and Luciano De La Iglesia for discussions and insights related to this work.

10. References

[1] Rao R P N 2013 *Brain-Computer Interfacing: An Introduction* (Cambridge University Press) ISBN 9780521769419

[2] Wolpaw J and Wolpaw E W 2012 *Brain-Computer Interfaces: Principles and Practice* (Oxford University Press)

[3] Moritz C T, Ruther P, Goering S, Stett A, Ball T, Burgard W, Chudler E H and Rao R P N 2016 *IEEE transactions on bio-medical engineering.* **63**(7) 1354–1367
[4] Lebedev M A and Nicolelis M A L 2017 *Physiological reviews* **97**(2) 767–837
[5] Walker E Y *et al.* 2019 *Nature Neuroscience* **22**(12) 2060–2065 URL https://doi.org/10.1038/s41593-019-0517-x
[6] Niparko J K 2009 *Lippincott Williams and Wilkins* (Oxford University Press)
[7] Weiland J D and Humayun M S 2014 *IEEE transactions on bio-medical engineering* **61**(5) 1412–1424
[8] Tomlinson T and Miller L E 2016 *Advances in experimental medicine and biology* **957** 367–388
[9] Tabot G A, Dammann J F, Berg J A, Tenore F V, Boback J L, Vogelstein R J and Bensmaia S J 2013 *Proceedings of the National Academy of Sciences* **110** 18279–18284 ISSN 0027-8424 (*Preprint* https://www.pnas.org/content/110/45/18279.full.pdf) URL https://www.pnas.org/content/110/45/18279
[10] Tyler D J 2015 *Current opinion in neurology* **28**(6) 574–581
[11] Dadarlat M C, O'Doherty J E and Sabes P N 2015 *Nature neuroscience* **18**(1) 138–144
[12] Flesher S N, Collinger J L, Foldes S T, Weiss J M, Downey J E, Tyler-Kabara E C, Bensmaia S J, Schwartz A B, Boninger M L and Gaunt R A 2016 *Science Translational Medicine* **8** 361ra141–361ra141 (*Preprint* https://www.science.org/doi/pdf/10.1126/scitranslmed.aaf8083) URL https://www.science.org/doi/abs/10.1126/scitranslmed.aaf8083
[13] Cronin J A, Wu J, Collins K L, Sarma D, Rao R P N, Ojemann J G and Olson J D 2016 *IEEE transactions on haptics* **9**(4) 515–522
[14] O'Doherty J, Lebedev M, Ifft P, Zhuang K, Shokur S, Bleuler H and Nicolelis M 2011 *Nature* **479**(7372) 228–231 URL https://doi.org/10.1038/nature10489
[15] Rao R P N 2019 *Current Opinion in Neurobiology* **55** 142–151
[16] Rao R P N 2020 Brain co-processors: Using AI to restore and augment brain function *Handbook of Neuroengineering* ed Thakor N (Springer)
[17] Yang Y, Qiao S, Sani O, Sedillo J, Ferrentino B, Pesaran B and Shanechi M 2021 *Nature Biomedical Engineering* **5**(4) 324–345 URL https://doi.org/10.1038/s41551-020-00666-w
[18] Tafazoli S, MacDowell C, Che Z, Letai K, Steinhardt C and Buschman T 2020 *Journal of Neural Engineering* **17** 056007 URL https://doi.org/10.1088/1741-2552/abb860
[19] Benabid A 2003 *Current opinion in neurobiology* **13**(6) 696–706
[20] Holtzheimer P and Mayberg H 2011 *Annual review of neuroscience* **34** 289–307
[21] Kisely S, Hall K, Siskind D, Frater J, Olson S and Crompton D 2014 *Psychological medicine* **44**(16) 3533–3542
[22] Fraint A and Pal G 2015 *Frontiers in Neurology* **6** 170 ISSN 1664-2295 URL https://www.frontiersin.org/article/10.3389/fneur.2015.00170
[23] Khanna P, Totten D, Novik L, Roberts J, Morecraft R and Ganguly K 2021 *Cell* **184**(4) 912–930 URL https://pubmed.ncbi.nlm.nih.gov/33571430/
[24] Bosking W, Beauchamp M and Yoshor D 2017 *Annual review of vision science* **3** 141–166
[25] Little S e a 2016 *Journal of neurology, neurosurgery, and psychiatry* **87**(7) 717–21
[26] Berger T W, Song D, Chan R H M, Marmarelis V Z, LaCoss J, Wills J, Hampson R E, Deadwyler S A and Granacki J J 2012 *IEEE transactions on neural systems and rehabilitation engineering : a publication of the IEEE Engineering in Medicine and Biology Society* **20**(2) 198–211
[27] Kahana M J e a 2021 *medRxiv* (*Preprint* https://www.medrxiv.org/content/early/2021/05/22/2021.05.18.21256980.full.pdf) URL https://www.medrxiv.org/content/early/2021/05/22/2021.05.18.21256980
[28] Bolus M, Willats A, Rozell C and Stanley G 2021 *Journal of neural engineering* **18**(3)
[29] Michaels J, Schaffelhofer S, Agudelo-Toro A and Scherberger H 2020 *Proceedings of the National Academy of Sciences* **117** 32124–32135 ISSN 0027-8424 (*Preprint* https://www.pnas.org/content/117/50/32124.full.pdf) URL https://www.pnas.org/content/117/50/32124
[30] Kim L Y, Harer J A, Rangamani A, Moran J, Parks P D, Widge A S, Eskandar E N, Dougherty

D D and Chin S P 2016 *2016 38th Annual International Conference of the IEEE Engineering in Medicine and Biology Society (EMBC)* 808–811

[31] Güçlü U and van Gerven M 2017 *Frontiers in computational neuroscience* **11**

[32] Sussillo D, Churchland M, Kaufman M and Shenoy K 2015 *Nature Neuroscience* **18**(7) 1025–1033

[33] Simonyan K and Zisserman A 2015 Very deep convolutional networks for large-scale image recognition *International Conference on Learning Representations*

[34] Puthenveettil S, Fluet G, Qiu Q and Adamovich S 2012 *Annual International Conference of the IEEE Engineering in Medicine and Biology Society. IEEE Engineering in Medicine and Biology Society. Annual International Conference* **2012** 4563–4566

[35] Loshchilov I and Hutter F 2017 *arXiv preprint arXiv:1711.05101*

[36] Dura-Bernal S, Li K, Neymotin S, Francis J, Principe J and Lytton W 2016 *Frontiers in Neuroscience* **10** 28 ISSN 1662-453X URL `https://www.frontiersin.org/article/10.3389/fnins.2016.00028`

[37] Castaño-Candamil S, Ferleger B I, Haddock A, Cooper S S, Herron J, Ko A, Chizeck H J and Tangermann M 2020 *Frontiers in Human Neuroscience* **14** 421 URL `https://www.frontiersin.org/article/10.3389/fnhum.2020.541625`

[38] Martens J and Sutskever I 2011 *Proceedings of the 28th International Conference on Machine Learning (ICML-11)* 1033–1040

[39] Kao J 2019 *Journal of Neurophysiology* **122** 2504–2521 URL `https://doi.org/10.1152/jn.00467.2018`

11. Supplementary Materials

11.1. Details of the simulated task.

The reach-to-grasp task on which the mRNN was trained involves multiple phases, which can be identified by the mRNN's inputs. Initially, the NHP subject sat in a dark room, with only a red cue visible. After a short period, an object was presented to the subject visually, after which the overhead light was turned off and once again only the red cue was visible. After another brief period, the red cue was turned off, which cued the subject to perform a grasp and hold of the object (still in the dark). This task is presented in more detail in the work of Susillo [32] and Michaels et al. [29].

The inputs to the mRNN network encode the task phase information. It consists of a twenty dimensional vector of visual features, which are presented only to the input (AIP) end of the network, and a 1D hold signal, which is presented to all neurons across the network. The authors of Michaels et al. [29] derived the hold signal from the grasp data, and it represents a point in time shortly before grasping began. As explained above, the visual features are drawn from VGGNet [33], based on rendered images. The images consist of some combination of the red cue light and the object image. Note that the visual input vector and hold signal are not observed directly by the co-processor, but rather indirectly via brain recordings.

The phases of the task are depicted in Table 1, and the timeline of a single trial is depicted in Fig. 14.

Description	**Cue**	**Object image**	**Hold signal**
A rest period, during which a red cue light is presented	On	Off	On
The object presentation period, during which the image of the object and cue are visible	On	On	On
A rest period	On	Off	On
Cue is turned off	Off	Off	On
Subject performs grasp	On	Off	Off

Table 1: Phases of the reach to grasp task. During each phase, a visual stimulus as well as a binary hold signal are presented. The visual stimulus encodes an image, consisting of a red cue light and/or an image of an object.

11.2. Training the grasping model network.

For our simulation, we leverage a pre-trained mRNN model, provided by the lead author of Michaels et al. [29], and used with their permission. The training method for that model is based on prior work by the same authors, and others [32].

Training involved the use of Hessian-free optimization [38], rather than the more common first-order stochastic gradient descent. Additionally, an L2 firing rate

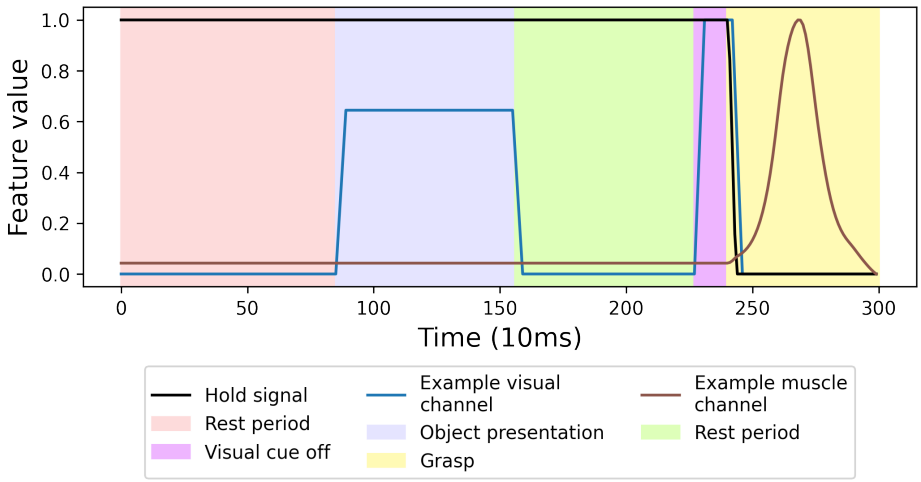

Figure 14: Timeline of a Single Trial

regularization, and an L2 input and output model weight regularization were used. These regularizations are believed to result in more biologically plausible RNNs [39].

The authors varied the model's nonlinearities, regularization weights, and inter-module sparsities. Among those, we chose one model arbitrarily for our study. Specifically, the model we chose was structured, and trained using:

- The rectified hyperbolic tangent nonlinearity
- 1e−1 Inter-module sparsity
- 1e−3 L2 firing rate regularization
- 1e−5 L2 weight regularization

11.3. EN/CPN Interleaving.

We train a CPN until an EN is no longer useful. At that point we train a new EN. We deem an EN as no longer useful if one of the following predicates becomes true:

- The EN prediction loss is greater than $min(6e{-}4, L/10)$, where L is the most recent task loss. EN prediction loss is an MSE loss between the EN's prediction of muscle trajectories, and the actual muscle trajectories output by the grasping model network.
- Task loss increased across 15 of the previous 30 training epochs.
- 100 CPN training epochs have elapsed.

Likewise, the EN training period ends when its prediction loss L on the validation data set drops below a threshold of $max(3e{-}4, L/50)$.

11.4. Sensor drift.

To simulate sensor drift, we add a vector to a bias term introduced to the recording function. We draw the elements of the vector from a zero-mean Gaussian distribution, with variance based on the mean value of the recording function from prior connection-lesion experiments. That allows us to put it into a reasonable range, where it is effective but not extreme. We attempted the experiment with several values of the variance, and found the results to be principally the same: the co-processor eventually learned, but at a rate slower than otherwise. We present results for a variance of 1.5e−3, which is 2% of the mean recording value.

11.5. Passthrough reference model.

To understand the effect of the recording and stimulation functions on the co-processor's performance, we repeated our experiment with the F5-M1 connection lesion and coadaptation, with passthrough recording and stimulation functions. "Passthrough" here means that the recording and stimulation functions have dimensionality equal to the number of neurons we are recording from or stimulating, respectively, and that there is no temporal or spatial smoothing used. That allows the co-processor to directly observe the hidden state of the AIP and F5 neurons in the simulated grasping circuit, and to directly influence the hidden state of the neurons in M1 it stimulates.

For this passthrough version of the experiment, we additionally increased the number of artifical neurons making up the CPN and EN, to account for the additional dimensionality of the inputs and outputs. Specifically, we increased the CPN from 61 to 200 neurons, and the EN from 87 to 351. We measured whether the increase in neurons alone caused in the different results we see here, and found it did not; we omit those results for brevity.

In Fig. 15 we see that the co-processor performed significantly better with the passthrough functions. It learned faster, and to a higher recovery level: 90% compared with 97%. Note: we truncate the results to the point we stopped the passthrough experiment. The reader can find the final results in Supplementary Materials 11.7.

11.6. Effect of observability on the recording function and training results.

To study the effect of brain observability on the co-processor's training behavior we repeated the co-adaptive connection lesion experiment (4.3) with varying recording functions. Here we varied the number of simulated electrodes in each mRNN module, and additionally performed an experiment with a passthrough recording function, as described in the prior section. Specifically, our original experiment used 20 electrodes per module. Our additional experiments include 1, 10, and 60 electrodes per module, and the passthrough recording function. This allows us to explore any gradient in the co-processor training results with respect to observability of the brain. Additionally, we reduced the variance of the Gaussian governing the sensor model, such that an

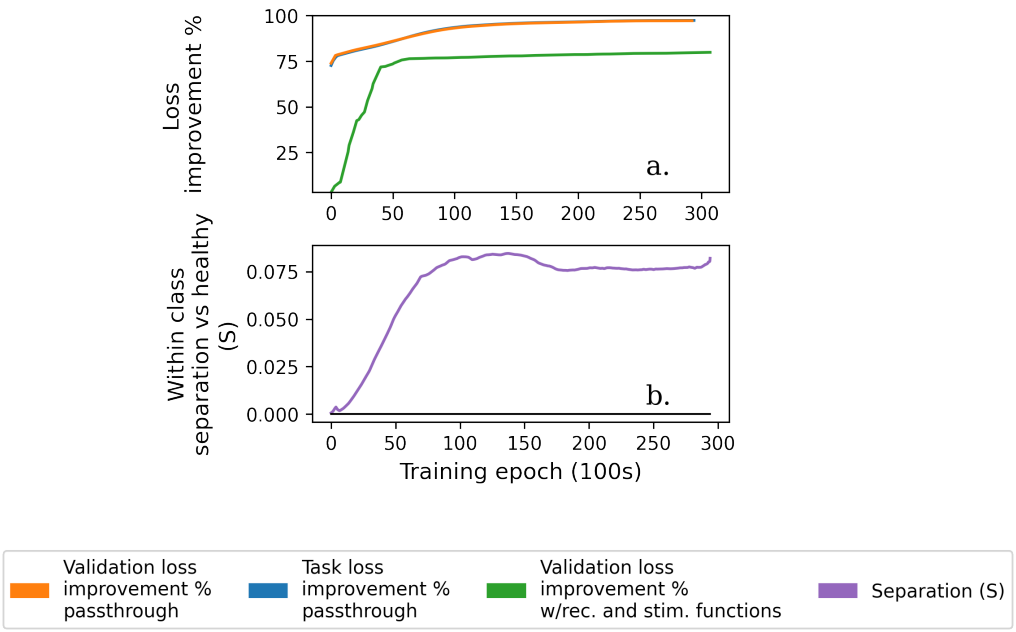

Figure 15: **Training Results: passthrough recording and stimulation functions.** The significantly faster training and higher recovery suggest the recording and stimulation functions make the task more difficult for the co-processor.

experiment with e.g. 1 electrode per module measures effectively only 1-2 neurons per module. We held the number of neurons making up the CPN and EN fixed across these variations to ensure we are examining the effects of the recording function alone. We continued to stop learning at the point of 90% recovery or a slow rate of recovery. In Fig. 16 we present the results.

We did not experiment with the placement of the electrodes, i.e. varying their location among the neurons. It wasn't necessary to do so for the purpose of this experiment. However, it's conceivable that results could improve considerably if we happened to observe a small handful of key neurons.

Overall, learning is effectively the same regardless of the recording function, up to the point that only a small number of neurons can be observed. In all cases except the case of a single electrode, the co-processor learned to improve task performance to the 90% recovery point. Some variation in learning efficiency occurred, and perhaps notably the experiments with 1, 10 electrodes observed the lowest two rates of recovery. The passthrough function and 60 electrode model observed the fastest recovery rates. Without additional computational power it remains difficult to hypothesis test the effect of electrode count against learning efficiency, but the results suggest that small variations in electrode count away from the count of 20 used in our main experiments would not cause drastically different results.

Class separation behavior remained largely the same across these variations. The one exception is the experiment involving only 1 electrode per module. In that case,

the co-processor slowly learned to treat the object classes similarly. That suggests that the classes could not be differentiated by the small amount of information attainable from a single electrode. In this case, the co-processor reduced towards a simpler closed-loop stimulator which modulates its behavior entirely on the user's volition to initiate movement, due to the hold signal being observable from every neuron.

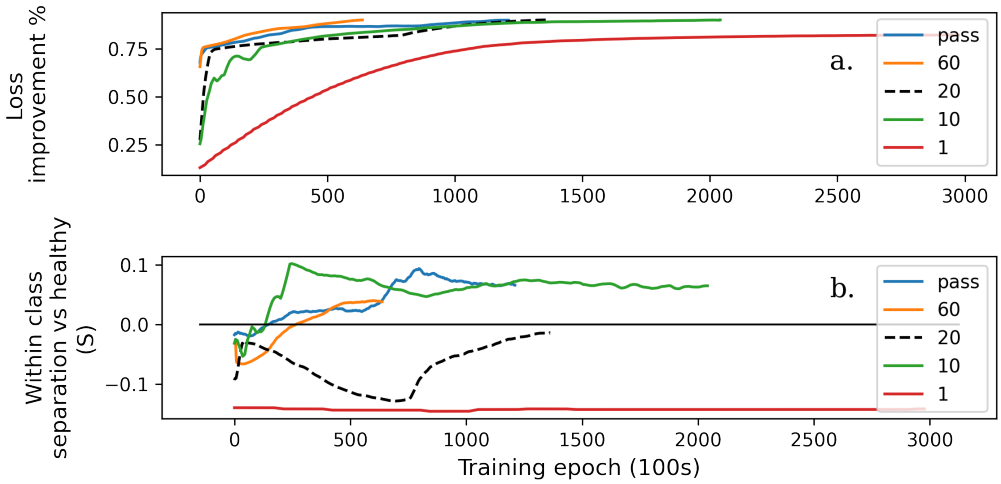

Figure 16: **Training Results: varying observability of the brain.** (a) Increasing observability of the brain leads to faster learning. Here we show results with a single simulated recording electrode in each module "1", compared with "20" electrodes for the results reported in the main portion of this paper, and compared with other electrode counts. "pass" refers to a passthrough recording function where every simulated neuron was directly measured. Note that learning is generally the same as observability increases, though perhaps somewhat faster. We did not hypothesis test that effect. In all cases except "1", learning reached our 90% recovery threshold where we stop training. (b) As in our connection-based lesion experiment above (4.3), class separation initially varied, then trended towards the separation exhibited by the healthy mRNN network. However, in the single electrode experiment "1", class separation steadily decreased, suggesting that the information necessary to perform class separation cannot be determined from the information available to the single electrode.

11.7. Table of losses and recovery.

Experiment	**Lesioned loss**	**Min task loss**	**Min task val loss**	**Pct recov**	**Pct recov val**
AIP No-coadapt	0.004507	0.004599	0.004658	-2.32%	-3.82%
AIP Coadapt	0.004507	0.001575	0.001502	74.41%	76.26%
M1 No-coadapt	0.021136	0.005765	0.005604	74.73%	75.51%
M1 Coadapt	0.021136	0.004772	0.004815	79.55%	79.35%
Con No-coadapt	0.020719	0.002584	0.002583	89.99%	89.99%
Con Coadapt	0.020719	0.002583	0.002405	89.99%	90.88%
Recovery*	0.003834	0.003105	0.003077	22.31%	23.16%
Sensor drift	0.020719	0.002966	0.002825	88.10%	88.83%
Passthrough	0.020719	0.001095	0.001132	97.37%	97.19%

Table 2: Losses and recovery. *Lesioned loss and percent recoveries based on the post-recovery values. "Coadapt" refers to co-adaptation. "Con" refers to F5-M1 connection lesions. "Recovery" refers to the experiment involving recovery prior to co-processor training. For further exploration of the results, see Results.